Mechanistic pathway of NP-polymer interface to engender nanoscale confinement

Guotong Wang,[1] Ruijie Wang,[1] Chengyuan Wang*,[2] Chun Tang*,[1]
Ying Luo,[1] Dunhui Xiao [3]

1. Faculty of Civil Engineering and Mechanics, Jiangsu University，No. 301 Xuefu Road, Zhenjiang, Jiangsu 212013, China
2. Zienkiewicz Centre for Computational Engineering, Faculty of Science and Engineering, Swansea University, Bay Campus, Swansea, Wales SA1 8EN, UK
3. School of Mathematical Sciences, Tongji University, Shanghai, P.R. China, 200092

Abstract Nanoparticle (NP)-polymer interface imposes the confinement effects on the surrounding polymer, which in turn impacts the bulk properties of nanocomposites. This study aims to identify the physical origin of the nanoscale confinement and reveal the pathway of the NP-polymer interface to produce the confinement effects. Herein, molecular dynamics simulations and theoretical analyses show clear evidence that the interfacial interaction generates a high compression in the polymer, which lead to an increased mass density and the upshift of glass transition temperature. This eventually triggers the redistribution of the polymer density partially via the orientation adjustment of the polymer chain segments.

Keywords: interfacial interaction, nanoscale confinement, high compression

Email: chengyuan.wang@swansea.ac.uk and tangchun@ujs.edu.cn

1. Introduction

Interfacial confinement in the nanocomposite [1-10] is a key issue that lies at the intersection of the nano-mechanics and polymer physics of the nanofiller-polymer interface. Existing studies however were mainly focused on the side of polymer physics where the density fluctuation, the variations in glass transition temperature and chain orientation were observed for the polymer confined by the nanoscale interface [1-10]. While it is widely held that interfacial confinement effects are engendered by the interfacial interaction there is still a lack of experimental or simulation evidence. In particular, the mechanistic connection between the interfacial interaction and the physical changes in the local polymer are not well understood. As stated in [1], "the general law to regulate the behaviour of polymers subject to the interfacial interaction have not yet been established for nanocomposite."

To bring out the theoretical advancement, the present study has addressed the long-standing issue from the unique perspective of the mechanical responses of the polymer to interfacial interaction. This opens the door to the mechanistic pathway of the interfacial interaction to impact the physics of the polymer around the interface. Herein, a gold nanoparticle (AuNP)-polyethylene (PE) interface was studied based on a cohesive model and molecular dynamics simulations (MDS) to characterize interfacial interaction, explore the interfacial confinement and reveal the role of the interfacial interaction in determining the confinement on the PE. A continuum mechanics model was then used to evaluate the mechanical responses of the PE to the interfacial interaction and understand how it finally leads to the nanoscale confinement.

2. Nanoscale confinement of the AuNP-PE interface

We shall first explore the confinement effects of the gold nanoparticle (AuNP)-polyethylene (PE) interface on the neighboring PE (Fig.S1). Based on MDS (Supporting Information S3) the mass density ρ profile is shown in Fig. 1(a) for the equilibrium AuNP-PE system, where Z_m is the radial coordinate of the AuNP-PE system and AuNP radius R_{np} is 2.5 nm. Thus Z_m= 2.5 nm represent the AuNP surface. A sinusoidal variation of ρ is found with the maximum density 1.47 g/cm^3, around 63% higher than the bulk value 0.9 g/cm^3 (PE simulations are shown in detail and validated in Supporting Information S4). The density variation then decays rapidly and reaches the bulk value at the place 0.23 nm from the AuNP surface, i.e., Z_m = 2.73 nm.

The spatial orientation of PE chain segments is then measured in Fig. 1(b) by the radial order parameter $P_2(Z_m)$ defined by $P_2(Z_m) = {}^1\!/_2(3\langle \cos^2\theta\rangle - 1)$ [2]. It is noted that as the positions of the PE chain segments move away from the AuNP surface to the PE inner surface (i.e., point A), the position of peak density (point B) and finally, the position of the first local minimum density (point C), their orientation shifts from the direction (P_2≈ -0.5) nearly parallel with the AuNP surface to the one (P_2 ≈ 0.05) close to the perpendicular direction of the AuNP surface. Such density oscillation and orientation changes of PE chain segment agree with previous observations in the proximity of NP-polymer interface [2, 3, 5].

The glassy transmission temperature T_g is also measured for the PE in (i) the narrow area between the dashed lines a and b (Fig.1(a)), where the peak density is found and (ii) a wide area bounded by the dashed lines *a* and *c* (Fig.1(a)). In Fig. 1(c), the specific volume (SV) of the PE is shown as a function of temperature *T*. T_g is then given by the intersection of the two straight lines obtained by fitting the SV-*T* curve at its two ends. Here, T_g of area *ab* is 310K that is 30 K above T_g = 280 K of bulk PE (Supporting

Information S4 and Fig.S5). T_g = 288 K of area *ac* is slightly higher than the bulk value but lower than T_g in area ab.

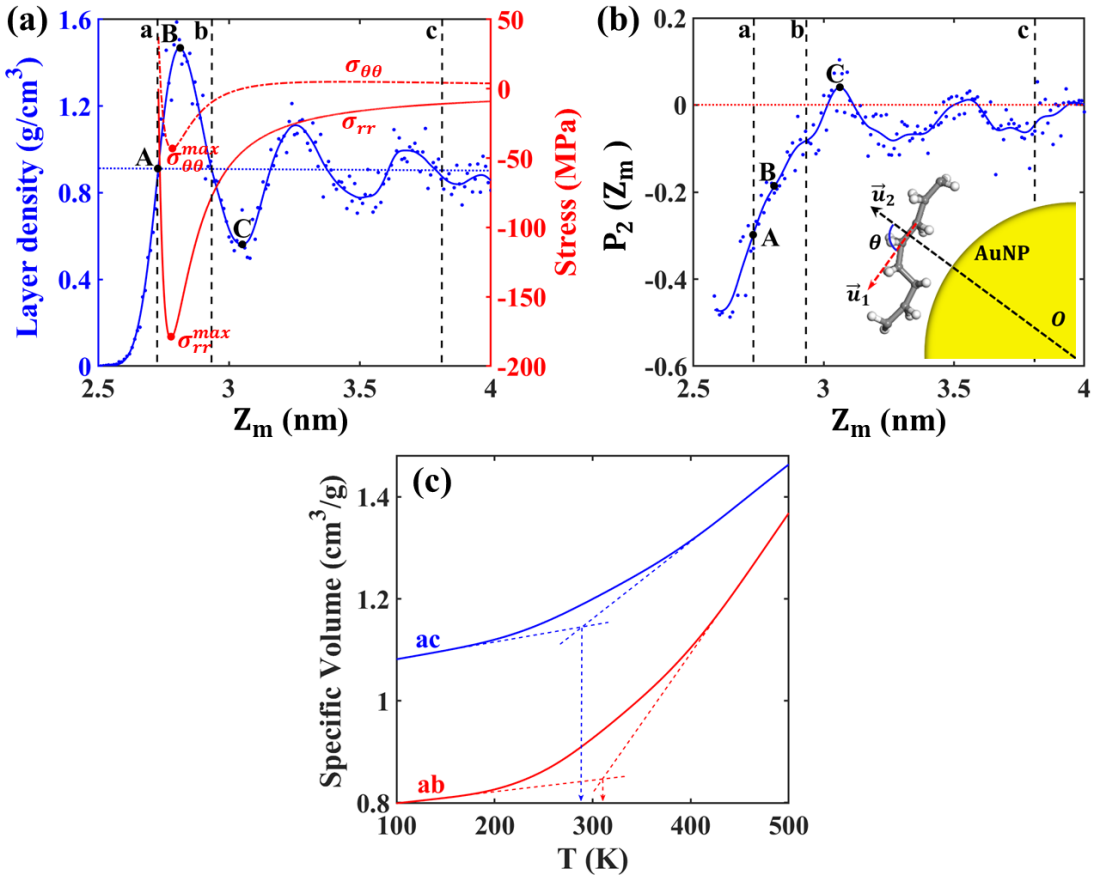

Fig. 1 (a) Mass density profile and normal stress distribution obtained for the local PE. Points A, B and C indicate the positions (Z_m) of the interface, the peak density and the first local minimum density. (b) Z_m – dependence of radial order parameter P_2 calculated for the C-C bonds on PE segments. The inset indicates the angle θ between a C-C bond vector $\vec{u}_1$ and $\vec{u}_2$. (c) Specific volume against the temperature T obtained in the area ab and ac shown in (a) and (b).

The confinement effects obtained in this section are thought to be a result of the interfacial interaction at the nanoscale [1]. The direct evidence however has not been reported. In particular, the pathway of the interfacial interaction to create the nanoscale confinement is still unclear.

3. Mechanical responses of PE to the interfacial interaction

To examine the issue raised above we shall investigate the mechanical responses of the PE to the interfacial interaction. A continuum mechanics model (Supporting Information S2) is used to obtain the local stress field induced by the vdW force in an equilibrium AuNP-PE system. Here, the PE is treated as an infinite elastic body with a spheric hole of radius $R_{np} + h_{eq}$ where h_{eq} is the radial gap between the AuNP surface and the inner surface of PE (ISP) at its equilibrium position. The PE is subjected to a vdW force $\frac{\partial \phi_{sur}}{\partial Z_m}$ (Fig. 2) due to the AuNP and ϕ_{sur} is the potential energy of the ISP (Supporting Information S1), which changes with ISP's position.

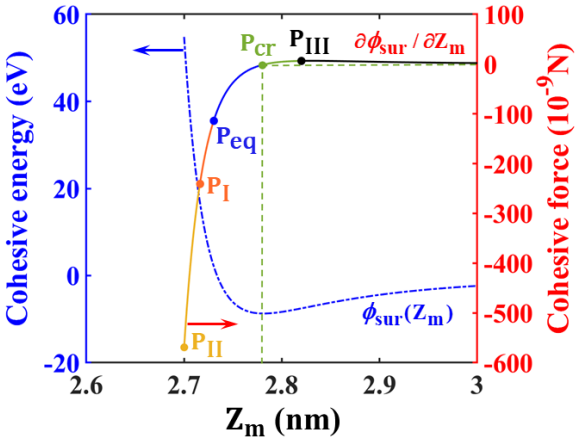

Fig.2 The radial distribution of ϕ_{sur} and $\frac{\partial \phi_{sur}}{\partial Z_m}$ on a PE surface with radius Z_m and surface density $\rho_m \times 1\dot{A}$.

The stress fields in the PE close to the AuNP-PE interface are shown in Fig.1 (a) where a compressive radial stress filed σ_{rr} is achieved. It rises rapidly to its maximum value σ_{rr}^{max} (~180 MPa) at the place 0.05 nm away from the ISP at $Z_m = R_{np} + h_{eq}$ $(i.e., 2.73\ nm)$. The compressive tangent stress $\sigma_{\theta\theta}$ is also achieved at the same place with the maximum value $\sigma_{\theta\theta}^{max} = 44$ MPa. Specifically, the location of $(\sigma_{rr}^{max},\ \sigma_{\theta\theta}^{max})$ is quite close to the place where the peak mass density is obtained (Fig.

1(a)). This implies the potential role of the compression (σ_{rr}^{max}, $\sigma_{\theta\theta}^{max}$) in generating the nanoscale confinement. Indeed, the pressure-induced mass density increase is reported for bulk polymer in recent studies [11]. It is thus of great interest to examine this issue for the PE confined by the AuNP-PE interface.

4. Physical origin of the nanoscale confinement

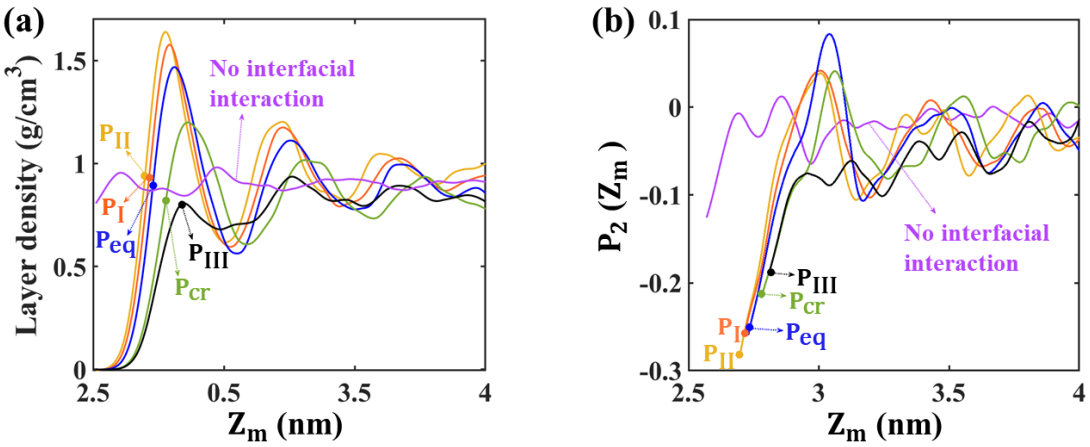

Fig.3 (a) Mass density and (b) radial orientation parameter P_2 obtained as the functions of Z_m for the local PE when the ISP is located at position P_{II}, P_I, P_{eq}, P_{cr} and P_{III}, respectively. The results obtained without the interfacial interaction are also shown.

To confirm the critical role of the interfacial interaction in the nanoscale confinement we shall first perform the MDS to achieve an equilibrium AuNP-PE system with the negligible interfacial interaction. The mass density profile of the PE and the orientation of their chain segments are then measured for such an AuNP-PE system in Fig. 3 (a) and (b), respectively. It is noted that the confinement effects observed in Fig.1 (a) and (b) vanish in the absence of the interfacial interaction. Almost constant density around the bulk value and P_2 close to zero are obtained in Fig.3 (b). The results clearly show that the confinement effects on the PE originate from the AuNP-PE vdW interaction.

Subsequently, an effort is made to reveal the pathway of the AuNP-PE interaction to

generate the confinement effects on the PE. Applying a hydrostatic compressive stress on the AuNP-PE system, we can push the ISP from its equilibrium position P_{eq} ($Z_m = R_{np} + h_{eq}$) to position P_I ($Z_m = R_{np} + h_1,\ h_1 < h_{eq}$) and then position P_{II} ($Z_m = R_{np} + h_2,\ h_2 < h_1$) closer to the AuNP surface ($Z_m = R_{np}$). In this process, the magnitude of the repulsive force $\frac{\partial \phi_{sur}}{\partial Z_m}$ on the ISP rises continuously (Fig. 2), which naturally leads to the constant improvement of ($\sigma_{rr}^{max},\ \sigma_{\theta\theta}^{max}$). As a result, in Fig.3(a) the peak mass density rises from 1.47 g/cm^3 for the equilibrium AuNP-PE system to 1.58 g/cm^3 for the system with the ISP at P_I and 1.64 g/cm^3 for the ISP at P_{II}.

On the other hand, applying a hydrostatic tensile stress can pull the ISP from its equilibrium interface P_{eq} away from the AuNP surface to position P_{cr} ($Z_m = R_{np} + h_{cr}$, $h_{cr} > h_{eq}$) where the repulsive $\frac{\partial \phi_{sur}}{\partial Z_m}$ on the ISP vanishes in Fig. 2. Hence, in Fig. 3(a) a decreased peak density 1.2 g/cm^3 corresponding to the ISP' position P_{cr} is obtained due to lower ($\sigma_{rr}^{max},\ \sigma_{\theta\theta}^{max}$). Further raising the hydrostatic tensile stress, we can pull the ISP further away from the AuNP surface to position P_{III} ($Z_m = R_{np} + h_{III},\ h_{III} > h_{cr}$). In this case, the vdW force acting on the PE becomes an attractive force (Fig. 2) and thus, the original compressive stress field in the PE will be replaced by a tensile stress field. Thus, in Fig. 3(a), the large mass density variation disappears and a nearly constant density around the bulk value is achieved for the PE. The analyses thus reveal the fact that the distributed vdW force on the PE induces a high compressive stress field that eventually leads to a large density increase of the PE.

It is noticed that both the mass density and T_g of the PE increase in area *ab* where ($\sigma_{rr}^{max},\ \sigma_{\theta\theta}^{max}$) are achieved (Figs.1(a) and (c)). The result is consistent with the experimental observation for bulk polymer [12] and the polymer confined by nanoscale interface [3, 5], which suggests that the high compressive stress ($\sigma_{rr}^{max},\ \sigma_{\theta\theta}^{max}$) should

be responsible for not only the density increase but also the rise of glassy transition temperature. The densified PE or the raised occupied volume in area *ab* (Fig. 1(a)) will result in the increased free volume or a lower density layer in the neighborhood and subsequently, next densified layer with raised occupied volume. Such a mass density redistribution is triggered by the maximum compressive stress and eventually results in the density oscillation of the PE in the proximity of the ISP.

Moreover, Fig.3 (a) and (b) show that no matter where the density change occurs there will be a shift of the PE chain orientation. When the ISP is moved to position P_{III} at $Z_m > R_{np} + h_{cr}$, the density variation from the ISP to the interior of the PE almost disappears (Fig. 3 (a)). At the same time, P_2 variation or the orientation shift of the PE chain segments nearly vanishes (Fig. 3(b)). This observation implies that the mass density redistribution caused by the compression (σ_{rr}^{max}, $\sigma_{\theta\theta}^{max}$) is likely realized via the orientation change of the PE chain segments.

4. Conclusion

This paper studies the AuNP-PE interface to reveal the physical origin of nanoscale confinement and mechanistic pathway to generate such effects on the polymer in the proximity of the interface.

It is found that for an equilibrium AuNP-PE system, the interplay between the interfacial interaction and the elasticity of the PE close to the interface results in a peak compressive stress of the order of the PE yield stress. It is this compressive stress that leads to a peak density and the upshift of the glass transition temperature T_g. The local upsurge of the density subsequently triggers a redistribution of PE density that finally develops into a sinusoidal variation partially via the orientation changes of the PE chain segments. The physical changes in the PE confined by the AuNP-PE interface thus

arise from the mechanical responses of the PE to the interfacial interaction.

The density and orientation changes of the PE confined by the interface may lead to the variation of its elastic modulus and energy barrier of electron tunnelling, which would eventually impact the elastic, electrical and piezoresistive properties of the nanocomposite. Specifically, the external loadings may enhance, weaken, or eliminate the confinement effects to eventually change the bulk properties of the nanocomposite.

Acknowledgement

This work is supported by the National Natural Science Foundation of China (Grant NO. 12072134).

References

[1] S. Napolitano, E. Glynos, N.B. Tito, Glass transition of polymers in bulk, confined geometries, and near interfaces, Rep. Prog. Phys. 80 (3) (2017) 036602.

[2] Z.K. Wang, Q. Lv, S.H. Chen, C.L. Li, S.Q. Sun, S.Q. Hu, Effect of Interfacial Bonding on Interphase Properties in SiO2/Epoxy Nanocomposite: A Molecular Dynamics Simulation Study, ACS Appl. Mater. Interfaces 8 (11) (2016) 7499-7508.

[3] D. Barbier, D. Brown, A.C. Grillet, S. Neyertz, Interface between End-Functionalized PEO Oligomers and a Silica Nanoparticle Studied by Molecular Dynamics Simulations, Macromolecules 37 (12) (2004) 4695–4710.

[4] J. Baschnagel, F. Varnik, Computer simulations of supercooled polymer melts in the bulk and in-confined geometry, J. Phys. Condens. Mat. 17 (32) (2005) 851–953.

[5] L. Chen, K. Zheng, X.Y. Tian, K. Hu, R.X. Wang, C. Liu, et.al., Double Glass Transitions and Interfacial Immobilized Layer in in-Situ-Synthesized Poly(vinyl alcohol)/Silica Nanocomposites, Macromolecules 43 (2) (2010) 1076–1082.

[6] M. Heydari-Meybodi, S. Saber-Samandari, M. Sadighi, 3D multiscale modeling to predict the elastic modulus of polymer/nanoclay composites considering realistic interphase property, Compos. Interface. 23 (7) (2016) 641-661.

[7] A.C. Genix, V. Bocharova, B. Carroll, M. Lehmann, T. Saito, S. Krueger, et.al., Understanding the Static Interfacial Polymer Layer by Exploring the Dispersion States of Nanocomposites, ACS Appl. Mater. Interfaces 11 (19) (2019) 17863–17872.

[8] S. A. Hosseini, S. Saber-Samandari, R. M. Moghadam, Multiscale modeling of interface debonding effect on mechanical properties of nanocomposites, Polym. Composite. 38 (4) (2017) 789-796.

[9] N. Das, N. Begam, M. Ibrahim, S. Chandran, V. Padmanabhan, M. Sprung, and J. K. Basu, Viscosity and Fragility of Confined Polymer Nanocomposites: A Tale of Two Interfaces, *Nanoscale* 11 (2019) 8546-8553

[10] A.J. Power, I.N. Remediakis, V. Harmandaris, Interface and Interphase in Polymer Nanocomposites with Bare and Core-Shell Gold Nanoparticles, Polymers 13 (4) (2021) 541.

[11] J. Pionteck, Determination of Pressure Dependence of Polymer Phase Transitions by pVT Analysis, Polymer 10 (6) (2018) 578.

[12] S. Bandi, D.A. Schiraldi, Glass Transition Behavior of Clay Aerogel/Poly(vinyl alcohol) Composites, Macromolecules 39 (19) (2006) 6537-6545.